STUDY OF ELECTRICITY AND HYDROGEN PRODUCTION IN A SOLID OXIDE FUEL CELL

Elisângela Martins Leal, elisangela.leal@vsesa.com.br
Demétrio Bastos Netto, demetrio.bastos@vsesa.com.br
Centro Tecnológico de Energia, Vale Soluções em Energia
Rodovia Presidente Dutra, km 138, Núcleo do Parque Tecnológico, Distrito de Eugênio de Melo, São José dos Campos, SP

Amauri Menezes Leal Junior, amaurileal@yahoo.com.br
Universidade Estadual Paulista, campus de Guaratinguetá
Av. Ariberto Pereira da Cunha, 333, Guaratinguetá, SP

Abstract. *This paper presents a model envolving a tubular solid oxide fuel cell with internal reforming. The model was developed using fluid dynamical, electrochemical and chemical mechanisms, heat and mass transfer principles using Matlab/Simulink® software. A geometrical resolution was included and the model was applied to predict dynamic variations of voltage, current and hydrogen co-production as the fuel cell responds to varying load demands. The results show that the model can be used to predict voltage and dynamic response characteristics of a SOFC as well as the co-production of hydrogen accurately and consistently for a variety of operating conditions.*

Keywords: *Solid Oxide Fuel Cell, hydrogen, electricity, dynamic modeling, environment.*

1. INTRODUCTION

Interest in hydrogen as a fuel has grown dramatically since 1990, and many advances in hydrogen production and utilization technologies have been made since then. Solid oxide fuel cells (SOFC) seem to be very promising for the direct conversion of chemical energy into electricity, attaining significantly higher efficiencies compared to similarly sized energy conversion devices, such as gas turbines and internal combustion engines, operated on natural gas. Furthermore, SOFCs yield high-temperature waste heat that can be used for cogeneration. The subject of this particular study is the analysis and investigation of how SOFC technology can be used to produce / co-produce electricity and hydrogen for other uses.

The main processes for hydrogen production are presented in several literature sources (Ahmed & Krumpelt, 2001; Ogden, 2002; Hammerli, 1984; Morse, 2004). Hydrogen production types include hydrocarbon-based processes (e.g., steam reforming, partial oxidation, gasification, catalytic decomposition), non-hydrocarbon-based processes (e.g., electrolytic, thermo-chemical, photochemical, photo-electrochemical) and integrated processes that may use renewable, nuclear, or other energy inputs. Steam-methane reforming is a very important and common industrial process for hydrogen production. Steam reformation produces a hydrogen-rich gas that is typically of the order of 70-75% hydrogen on a dry basis, along with 2-6% of methane, 7-10% of carbon monoxide, and 6-14% of carbon dioxide (Lipman, 2004). Typical hydrogen production plants purify the hydrogen rich stream after steam reformation through pressure swing absorption (PSA) or other purifying device.

The hydrogen economy, and in particular the use of hydrogen as an energy carrier for transportation applications, will depend upon local consumer access to inexpensive and environmentally sensitive pure hydrogen product delivery. Since hydrogen is challenging to store with high energy density, the transport, distribution and dispensing of hydrogen typically involves a significant energy and environmental impact. In addition, the infrastructure required for transport, distribution and dispensing is likely to be expensive and it will require several decades to introduce. Thus, attention must be paid to developing a means of providing hydrogen to consumers in an environmentally sensitive manner.

One environmentally sensitive means of addressing both local generation of power and the production and distribution of hydrogen is to co-produce hydrogen and electricity using a high temperature stationary fuel cell system. Internal reforming high temperature fuel cells, such as solid oxide fuel cells and molten carbonate fuel cells, are well developed technologies with a few commercial products available. These systems do not require hydrogen; they are instead directly fuelled by natural gas or renewable fuel such as landfill or digester gas. The natural gas is reformed either indirectly or directly in the anode compartment to produce hydrogen. Direct reformation results in both promoting hydrogen production and providing needed cooling to the fuel cell stack. Indirect reformation occurs in a separate but thermally integrated reactor. Significantly, these fuel cell systems do not electrochemically consume all the fuel that is supplied (a fundamental limitation) and they yield enough heat to reform much more than the amount of hydrogen they consume.

The literature shows the thermodynamic and electrochemical analyses of solid oxide and molten carbonate fuel cells used for the electricity and hydrogen production (Leal & Brouwer, 2006; Leal & Brouwer, 2005a; Leal & Brouwer, 2005b; Vollmar et al., 2000). In this work, a model with a solid oxide fuel cell is presented using a Matlab/Simulink® software. The fuel cell heat is used to drive hydrogen production in an endothermic reformer using internal reforming strategy.

2. SOLID OXIDE FUEL CELL (SOFC)

SOFC technology is promising for use in power generation applications, attaining significantly higher efficiencies compared to similarly sized energy conversion devices, such as gas turbines and internal combustion engines, when operated on natural gas. Furthermore, SOFCs produce high-temperature waste heat that can be used for cogeneration, which in this particular case is used to produce hydrogen for other uses.

Independent of the fuel used in an SOFC with an oxygen-ion-conducting electrolyte (the most common today), its operating principle relies on the continuous supply of fuel, containing hydrogen, carbon monoxide and methane or other hydrocarbons, to the anode compartment while the cathode is supplied with air. The reactions that occurs at the anode and cathode are, respectively (Larminie & Dicks, 2003):

$$H_2 + O^{2-} \rightleftharpoons H_2O + 2e^- \tag{1}$$

$$\tfrac{1}{2} O_2 + 2e^- \rightleftharpoons O^{2-} \tag{2}$$

Various fuel options are considered feasible for SOFC operation, especially after an appropriate external process in order to obtain a gas mixture that is rich in hydrogen, such as steam reforming. The electrochemically active species are H_2, CO and CH_4, but it is common in system-analysis practice to assume that only H_2 contributes to power generation while CH_4 is consumed through *in situ* steam reforming, providing additional amounts of H_2 and CO. The CO is consumed through *in situ* water-gas-shift reactions, providing additional amounts of H_2 (EES, 2002).

2.1. Cell Voltage

The equilibrium cell potential (E_{eq}) of a fuel cell in terms of temperature and gas compositions is given by the Nernst equation (EES, 2002):

$$E_{eq} = E^0 + (RT/n\,F)\ln\left(p_{H_2}\, p_{O_2}^{0.5} \big/ p_{H_2O}\right) \tag{3}$$

Where: R is universal constant [8.314 kJ.kmol^{-1}.K^{-1}], T is operating temperature [K], F is the Faraday constant [96,485 kC.kmol^{-1}], n is the number of electrons released by the chemical reaction [mol e^-/mol], p_i is the partial pressure of the specie i [Pa]. The Nernst equation provides a relationship between the ideal standard potential (E^0) for the cell reaction and the ideal equilibrium potential for given local temperatures and partial pressures of reactants and products. Fuel cell irreversible losses (caused by electrochemical dynamic limitations, as in activation polarization, or by mass transport limitations, or resistive heating) are estimated through local calculation of the three primary bulk losses of activation, concentration, and Ohmic polarizations (EES, 2002):

$$V_{cell} = E - \eta_{act} - \eta_{conc} - \eta_{Ohm} \tag{4}$$

Where: V_{cell} is the cell voltage under load [V]; η_{act} the activation polarization [V]; η_{conc} the concentration polarization [V]; and η_{Ohm} the Ohmic polarization [V]. Polarization losses are generally dependent on gas partial pressures, temperature, and current density, all of which are spatially distributed in an actual cell. Several approaches for calculating these polarization losses have been presented in the literature. One approach is to derive the activation polarization and the concentration polarization from the Butler-Volmer equation. Ohmic polarization was derived from Ohm's Law. Therefore, the activation, concentration and Ohmic polarization equations are, respectively (EES, 2002):

$$\eta_{act} = (RT/\alpha\, n\, F)\ln(j/j_0) \qquad \eta_{conc} = (RT/n\,F)\ln(1 - j/j_L) \qquad \eta_{Ohm} = j\,R_{int} \tag{5}$$

Where j_L is the limiting current density [A.m^{-2}], j_0 is the exchange current density [A.m^{-2}], α is the transfer coefficient [-], and R_{int} the internal resistance of the fuel cell [Ω.m^2], which can be calculated by (Chan et al., 2002):

$$R_{int} = (a/A)\exp\left(b/T\right)\delta \tag{6}$$

where a and b are specific constants of each material (given by Table 1), A is the geometrical area [m^2] and δ is the equivalent thickness of diffusion layer. According to Costamagna et al. (1998) and Virkar et al. (2000), the exchange current density can be calculated by:

$$j_0 = A\, e^{B/T} \tag{7}$$

Where A and B are intrinsic constants of the electrocatalyst used. Each polarization term and the voltage of the fuel cell were calculated using the parameters shown in Tables 1 and 2.

Table 1. Components characteristics of SOFC (EES, 2002; Chan et al., 2001; Virkar et al., 2000).

	Anode	**Electrolyte**	**Cathode**	**Interconnector**
Material →	***Ni/YSZ***	***YSZ***	***LSM/YSZ***	***Mg/LaCrO$_3$***
a [Ω.m^3]	2,98.10^{-5}	2,94.10^{-5}	8,11.10^{-5}	1,259.10^{-3}
b [K]	-1392	10350	600	4690
Thickness				
Anode supported [m]	7,5.10^{-4}	4,0.10^{-5}	5,0.10^{-5}	1,0.10^{-4}
Cathode supported [m]	1,5.10^{-4}	4,0.10^{-5}	2,0.10^{-3}	1,0.10^{-4}
Electrolyte supported [m]	1,5.10^{-4}	1,0.10^{-4}	5,0.10^{-5}	1,0.10^{-4}

Table 2. Others parameters for the SOFC system (Larminie & Dicks, 2003; Chan et al., 2002, EES, 2002).

Parameters	**Value**
Initial operating temperature (T)	1273 K
Initial operating pressure (P)	101,325 kPa
Electrons transferred in the reaction (n)	2
Transfer coefficient (α)	0.5
Porosity (ε)	30 %
Tortuosity (ξ)	6

2.2. Model Formulation

A tubular solid oxide fuel cell is modeled using discrete volumes assuming a well-stirred reactor. The total cell is axially discretized into 10 volumes, each one comprised of smaller sub-volumes representing the air supply pipe (ASP) with its associated gas volume, anode gas compartment, electrolyte and cathode compartment. An axis-symmetric orientation is utilized for calculation purposes and the model is one-dimensional in the axial direction. Gas flows in a co-flow arrangement in the anode and cathode; counter-flow with respect to incoming air in the ASP. The geometry is pictured in Fig. 1.

Heat is transferred between gases and solids by convection as well as axially through the solid by conduction. Also provisions are taken for radiant heat transfer from solid to solid, due to the high operating temperatures of SOFCs. Figure 2 displays a heat transfer network within the fuel cell. Parameters such as lengths, widths, material properties, and electrochemical data can be customized for various applications.

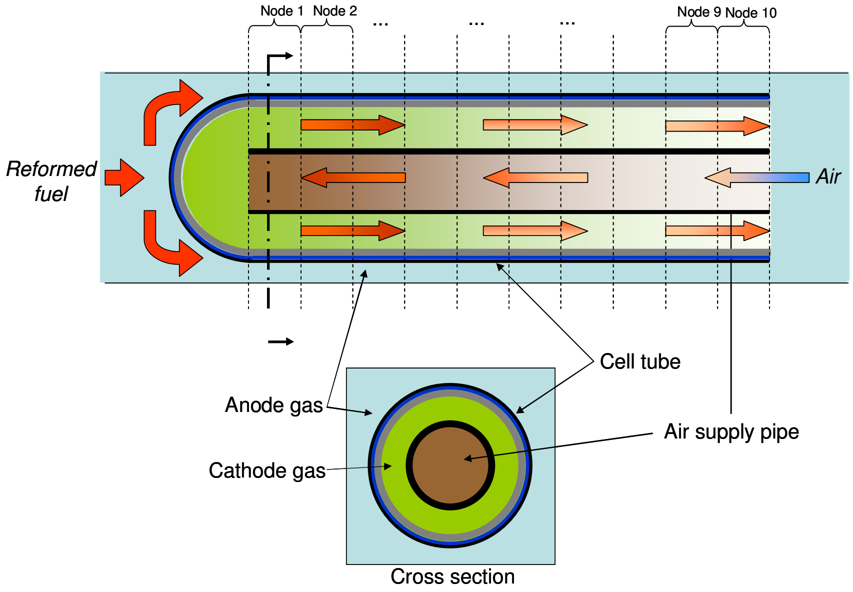

Figure 1. Geometrical model of the tubular SOFC.

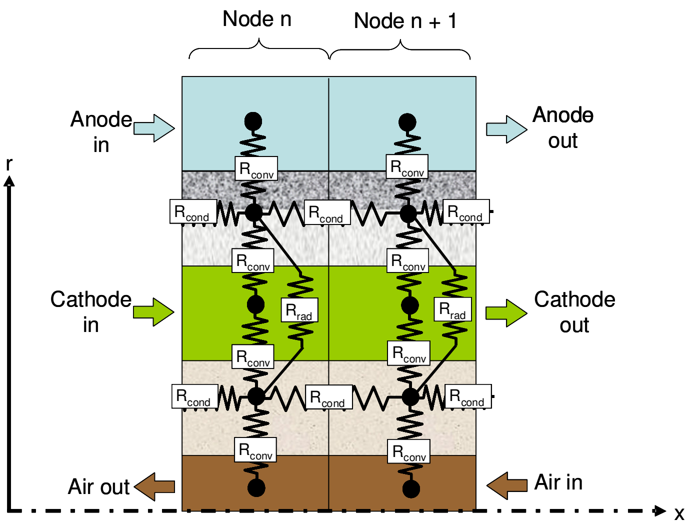

Figure 2. Heat transfer equivalent circuit.

The electrochemistry in the cell is modeled as a quasi-steady process in which the electrochemical-kinetics is assumed to take place at a rate much faster than the transport and heat transfer model dynamics. So the reactions are assumed to happen instantaneously at the electrolyte surface and to be complete. Diffusion times to the active sites in the electrolyte matrix are also assumed to be of the same order as the chemical kinetics and are neglected. With these assumptions, the species consumption and production rates become whole dependent on the current produced from the cell. At any point in time then, the local current production depends upon local bulk species concentrations in the anode and cathode compartments, an iteratively determined cell voltage (using an electrode equipotential assumption) and the local polarizations. A relatively simple mass/species balance equation for species conservation is thereby obtained (Gemmen et al., 2000):

$$\forall\left(\mathrm{dC}_k / \mathrm{dt}\right) = N_{k,\mathrm{in}} - N_{k,\mathrm{out}} + R_{\mathrm{p}} \tag{8}$$

Where $\forall$ is the finite control volume [m^3]; C_k is the individual concentration of species k [kmol.m^{-3}]; N_k, is the molar flow of species k [kmol.s^{-1}] and R_p is the total production rate [kmol.s^{-1}]. The energy balance in the cathode compartment can be written as (Achenbach, 1994):

$$\forall\left[\mathrm{d}(\rho\ \mathrm{E})/\mathrm{dt}\right] = \sum \mathrm{m}_{\mathrm{in}} \mathrm{E}_{\mathrm{in}} - \sum \mathrm{m}_{\mathrm{out}} \mathrm{E}_{\mathrm{out}} - Q_{\mathrm{conv,e}} - Q_{\mathrm{conv,ASP}} + Q_{\mathrm{rad}} + Q_{\mathrm{gen}} \tag{9}$$

Where E denotes energy [kJ.kg^{-1}], m is mass flux (the subscripts in and out denote into and out of the control volume) [kg/s], Q_{conv} is the convective heat transfer in the electrolyte (subscript e) and at the air supply pipe [kW], Q_{rad} is radiation heat transfer [kW] and Q_{gen} is the generation of heat [kW] due to the chemical reaction, which can be calculated by (Achenbach, 1994):

$$Q_{\mathrm{gen}} = j\left[\left(\Delta \mathrm{H}^{\mathrm{f}}_{\mathrm{H_2O}} / n\ \mathrm{F}\right) - \mathrm{V}_{\mathrm{cell}}\right] \tag{10}$$

The equations used for the conduction, convection and radiation heat transfer are as follow (Incropera & DeWitt, 1998):

$$Q_{\mathrm{cond}} = \frac{\mathrm{k}\ \mathrm{A}_{\mathrm{cond}}}{L} \Delta \mathrm{T} \qquad Q_{\mathrm{conv}} = h\ \mathrm{A}_{\mathrm{conv}} \Delta \mathrm{T} \qquad Q_{\mathrm{rad}} = \varepsilon \mathrm{A}\ \sigma\left(\mathrm{T}^4_{\mathrm{se}} - \mathrm{T}^4_{\mathrm{g(cat)}}\right) \tag{11}$$

Where A_{cond} is the flux area [m^2], k is the thermal conductance of the material the heat flux is going through [kW.m^{-1}.K^{-1}], L is the distance between the bulk temperature differences [m], h is the convective heat transfer coefficient [kW.m^{-2}.K^{-1}], A_{conv} is the surface area [m^2], ε is the emissivity [-], σ is the Stefan-Boltzmann's constant [5,67x10^{-11} kW.m^{-2}.K^{-4}], T_{se} is the temperature in the electrolyte surface [K] and $T_{\mathrm{g(cat)}}$ is the temperature of the cathode gas [K].

3. STEAM REFORMING

Steam reforming and water-gas shift reactions occur simultaneously to the electrochemical reactions in the SOFC anode compartment. The conservation equations of mass, species, momentum and energy are also applied to the reformer module. The reformer model considers the chemical kinetics of the following reactions (EES, 2002):

$$CH_4 + H_2O \rightarrow CO + 3H_2 \tag{12}$$

$$CO + H_2O \rightarrow CO_2 + H_2 \tag{13}$$

$$CH_4 + 2H_2O \rightarrow CO_2 + 4H_2 \tag{14}$$

The reaction rates of the steam reforming reaction (12) and water/gas shift reaction (13) were determined by the Arrhenius equation. The model uses the rates that are consistent with the use of nickel-based catalysts. The reaction rate equation of reactions (12), (13) and (14) can be written as (Xu & Froment, 1989):

$$r_{12} = \left(k_{12}/\mathrm{DEN}^2\right)\left[\left(P_{CH_4}P_{H_2O}/P_{H_2}^{2,5}\right) - \left(P_{CO}P_{H_2}^{0,5}/Kp_{12}\right)\right] \tag{15}$$

$$r_{13} = \left(k_{13}/\mathrm{DEN}^2\right)\left[\left(P_{CO}P_{H_2O}/P_{H_2}\right) - \left(P_{CO_2}/Kp_{13}\right)\right] \tag{16}$$

$$r_{14} = \left(k_{14}/\mathrm{DEN}^2\right)\left[\left(P_{CH_4}P_{H_2O}^2/P_{H_2}^{3,5}\right) - \left(P_{CO_2}P_{H_2}^{0,5}/Kp_{14}\right)\right] \tag{17}$$

The denominator (DEN) used in equations (15) and (16) is (Xu & Froment, 1989):

$$\mathrm{DEN} = 1 + K_{CO}P_{CO} + K_{H_2}P_{H_2} + K_{CH_4}P_{CH_4} + K_{H_2O}P_{H_2O}/P_{H_2} \tag{22}$$

According to Arrhenius and Van't Hoff equations, the reaction constants k_m (m = 12, 13, 14) and K_n (n = CO, CH_4, H_2O, H_2) in the above equations can be calculated by the exponentials factors (A_m and A_n) and the absorption parameters (E_m and ΔH_n) of the following equations (Xu & Froment, 1989):

$$k_m = A_m \exp\left(-\frac{E_m}{\mathrm{RT}}\right) \qquad K_n = A_n \exp\left(-\frac{\Delta H_n}{\mathrm{RT}}\right) \tag{23}$$

Table 3 exhibits the constants used in the model. It is assumed that the carbon monoxide is consumed only in the water/gas shift reaction (13) and produced by the steam reforming (12).

Table 3. Reformer model constants (Weber et al., 2002).

Constants	Activation energies [kJ.mol^{-1}]	Preexponential factors
k_{12}	240,1	1,366 x 10^{15} [kmol . MPa^{0,5} . kgcat^{-1} . h^{-1}]
k_{13}	67,13	1,955 x 10^{7} [kmol . MPa^{-1} . kgcat^{-1} . h^{-1}]
k_{14}	243,9	3,220 x 10^{14} [kmol . MPa^{0,5} . kgcat^{-1} . h^{-1}]
Constants	**Adsorption heats [kJ.mol^{-1}]**	**Preexponential factors**
K_{CO}	-70,65	8,23 x 10^{-4} [MPa^{-1}]
K_{CH4}	-38,28	6,65 x 10^{-3} [MPa^{-1}]
K_{H2O}	88,68	1,77 x 10^{5} [-]
K_{H2}	-82,90	6,12 x 10^{-8} [MPa^{-1}]
Equilibrium constants		
Kp_{12} = 1,198 x 10^{11} exp(-26830/T) [MPa]^2		
Kp_{13} = 1,77 x 10^{-2} exp(4400/T) [MPa]^0		
Kp_{14} = Kp_{12} Kp_{13} [MPa]^2		

When the reformer was modeled, each module was built to either be integrated with the system as a whole or to be used separately, in order to be assessed in both ways. For simulation purpose, the reformer module was divided into five equal nodes along the length in order to capture longitudinal variations. A node sensitivity analysis showed that, in this case, the reformer model needed to be divided into five nodes in order to achieve the desired accuracy. The use of more than five nodes only provides small gains in accuracy with a large increase in computation time. The reformer module consists of five subsystems: catalytic bed, gas fuel, exhaust gas, reformed gas and mixture of gases.

4. DISCRETIZATION

A tubular solid oxide fuel cell is modeled using discrete volumes assuming a well-stirred reactor mode. The total cell is discretized axially into 10 volumes, each comprised of smaller sub-volumes representing the ASP with its associated gas volume, the anode gas compartment, the electrolyte, and the cathode compartment. An axis-symmetric orientation is utilized for calculation purposes and the model is one-dimensional in the axial direction. Gas flows in a co-flow arrangement in the anode and cathode and as counter-flow with respect to the incoming air in the ASP (see Figure 1).

Along the length of the cell, a global equal-potential condition is enforced, i.e., the voltage across the cell throughout all nodes is constant and is also the overall cell voltage. As a result, at each node the following electrochemical relation applies (Roberts et al., 2003):

$$V_{cell} = \sum_{node} j_{node} R_{load} \tag{29}$$

The exhaust gases of the fuel cell is used to drive the reformer in order to produce hydrogen. The model was developed in MATLAB Simulink® (Simulink/MATLAB, s.d.). This was selected because of its dynamic solution capabilities, a flexible and versatile user interface, and especially, compatibility with dynamic control system development. The model was constructed in a physically representative manner, i.e., separate graphical components representing the anode, cathode, etc., for each of the model nodes, allowing easy visualization and debugging.

5. RESULTS AND DISCUSSION

The polarization curve represents the voltage and current characteristics of the electrochemical reaction that occurs inside the fuel cell. Figure 3 shows the results of the IR-SOFC model for voltage, current and power generated by the fuel cell, for an increase in current from 160 A to 225 A (about 40%). The model converges towards a reasonable solution. The curve shows the ohmic predominant region, i.e. the region where the materials characteristics of the SOFC overlap.

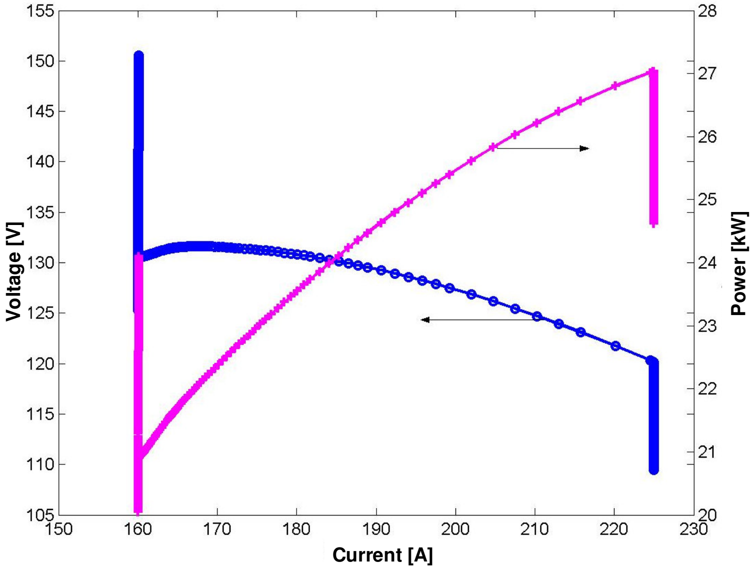

Figure 3. Results of voltage and power *versus* current.

Generally, when a fuel cell experiences a load change it responds with a quick electrochemical and transport transient and a slower thermal response. Since most of the physical and chemical processes that govern a fuel cell operation are strongly temperature dependent, as well as the thermal transient affects cell voltage and current. In a typical system, these thermal transients can have large time constants (e.g., 100’s to 1000’s of seconds) due to the relatively large thermal mass of a fuel cell. Figure 4 shows the electrochemical behavior of the fuel cell for a 40% current perturbation. This figure shows the behavior before and after the perturbation in current on the cathode temperature, Nernst potential, activation and concentration polarizations. It is observed that the temperature transient is longer than the Nernst potential and polarizations. Comparing the Nernst potential to the activation and concentration polarizations, the Nernst potential is longer and has a peak in the potential due to the electrochemical and material response adjustment in time. This behavior is the same verified by Mench et al (2003a, 2003b).

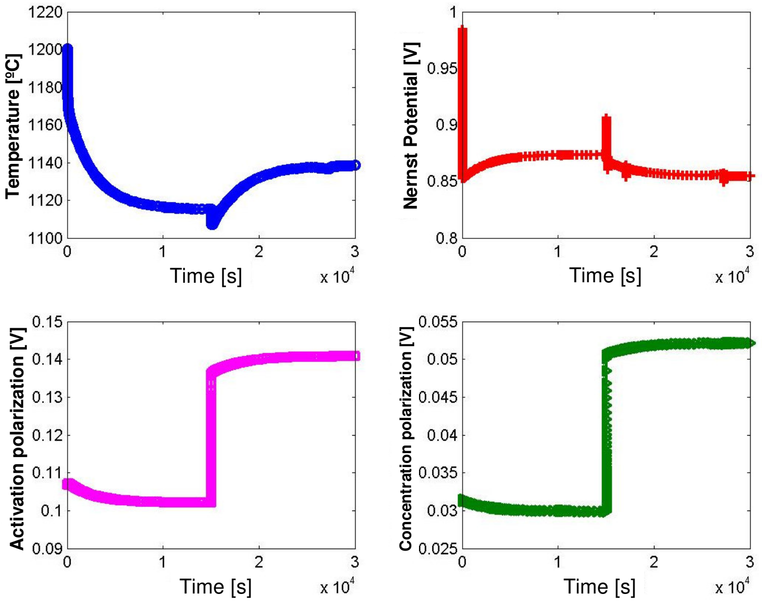

Figure 4. Results of fuel cell electrochemical behavior.

Figure 5 shows the production of hydrogen by the reformer in steady state (Figure 5a) and dynamic state (Figure 5b). It can be observed that the hydrogen production decreases when the current and consequently the temperature of the fuel cell increases. According to Figure 5a (steady state analysis) the production of hydrogen decreases with the increase of temperature from 800ºC. Solid oxide fuel cell operating temperature is 1000ºC, which is the initial condition of the model. The temperature increase due to current increase causes a drop in the hydrogen production by the reformer as predicted in theoretical results.

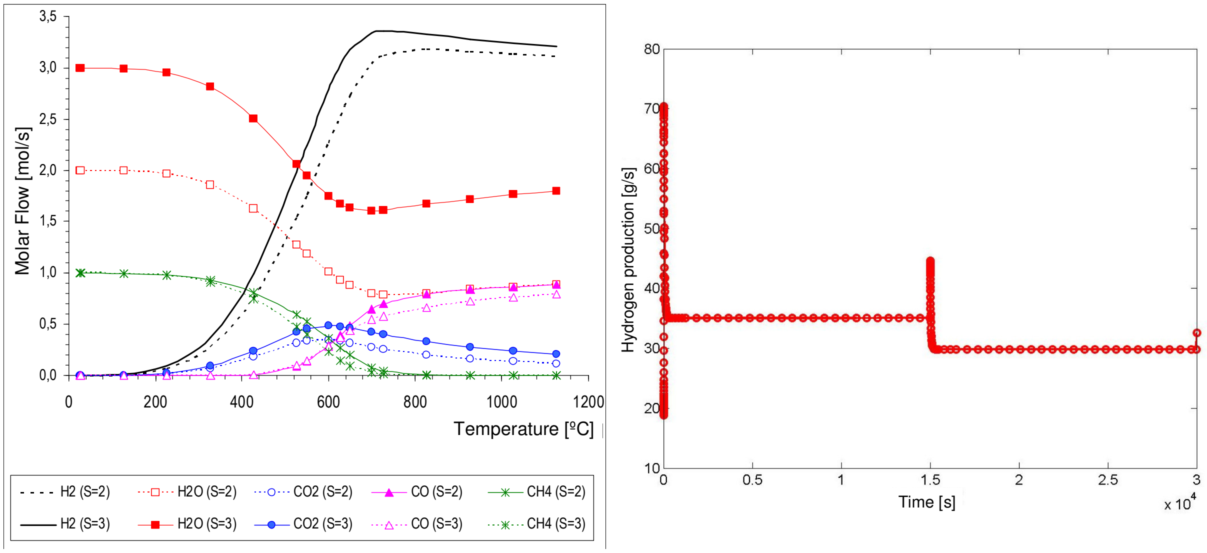

(a) Steam to carbon ratio (S) of 2 and 3

(b)

Figure 5. Hydrogen production: (a) steady state analysis and methane as the fuel, and (b) dynamic analysis with a 40% perturbation in the fuel cell current

6. CONCLUSIONS

The prediction of fuel cell performance can be obtained experimentally or from theoretical models. An experimental research is time consuming and is an expensive process because there is a need to acquire or to manufacture the device. On the other hand, theoretical models can be quick and cheap to achieve but they depend on the experimental validation in order to obtain a useful model. The operation of fuel cell dynamic systems is a complex process and includes, for example, interactions among the electrochemical processes as well as the heat and mass transfer processes. As a result, precise and reliable models that can capture the dynamic behavior as well as identify the thermal gradients of the fuel cell are highly desirable. In this work, a fuel cell modeling in Matlab/Simulink® environment were presented, using the principles of fluid dynamics, electrochemistry and chemistry mechanisms and the heat and mass transfer processes that govern a tubular SOFC. A geometric representation axially one-dimensional and longitudinally two-dimensional was applied to predict the dynamic variations of voltage, current, power and hydrogen co-production when the fuel cell responds to changes in load or current. Simulations were conducted to verify the model performance. The results showed that the model converges towards a reasonable solution. It was observed that the temperature transient is longer than the Nernst potential. Regarding to the hydrogen co-production, the results showed that the production of hydrogen decreases when the current and, consequently, the cell fuel temperature increases, which is confirmed by the steady state analysis presented. The analyses performed here showed that the simulation of the first principles using simplified geometry may be useful to obtain knowledge of the response characteristics and dynamic behavior of fuel cells. The future use of such models can be especially valid for more detailed simulations.

7. ACKNOWLEDGEMENTS

The authors would like to acknowledge FAPESP (Fundação de Amparo à Pesquisa do Estado de São Paulo, Brazil, Processo 2005/55375-2) for the financial support in this project.

8. REFERENCES

Ahmed, S., Krumpelt, M., 2001, "Hydrogen from hydrocarbon fuels for fuel cells", International Journal of Hydrogen Energy, 26, pp. 291–301

Chan, S.H., Khor, K.A., Xia, Z.T., 2001, "A complete polarization model of a solid oxide fuel cell and its sensitivity to the change of cell component thickness", Journal of Power Sources, 93, pp. 130-140.

Chan, S.H., Low, C.F., Ding, O.L., 2002, "Energy and exergy analysis of simple solid-oxide fuel-cell systems", Journal of Power Sources, 103, pp. 188-200.

Chan, S.H., Xia, Z.T., 2002, "Polarization effects in electrolyte/electrode-supported solid oxide fuel cells", Journal of Applied Electrochemistry, 32, pp. 339–347.

Costamagna, P., Costa, P., Antonucci, V., 1998, "Micro-modelling of solid oxide fuel cell electrodes" Electrochimica Acta, 43 (3-4), pp. 375-394

EES - Energy and Environmental Solutions, National Energy Technology Laboratory, 2002, "Fuel Cell Handbook Sixth Edition". U.S. Department of Energy.

Hammerli, M., 1984, "When will electrolytic hydrogen become competitive?" International Journal of Hydrogen Energy, 9 (1/2), pp. 25-51.

Kanamura, K., Yoshioka, S., Takehara, Z., 1991, "Dependence of entropy change of single electrode on partial pressure in solid oxide fuel cell" Journal of the Electrochemical Society, 138 (7), pp. 2165-2168.

Larminie, J., Dicks, A., 2003, Fuel Cell Systems Explained, England: John Wiley and Sons, Inc.

Leal, E. M.; Brouwer, J., 2005b, "A thermodynamic analysis of electricity and hydrogen co-production using a solid oxide fuel cell". In: Proceedings of the 3rd International Conference on Fuel Cell Science, Engineering and Technology, 2005, Ypsilanti, MI. American Society of Mechanical Engineers, v. CD-ROM.

Leal, E. M.; Brouwer, J., 2006, "A thermodynamic analysis of electricity and hydrogen co-production using a solid oxide fuel cell". Journal of Fuel Cell Science and Technology, Vol. 3(2), pp. 137-143.

Leal, E.M.; Brouwer, J., 2005a, "Production of hydrogen using high-temperature fuel cell: energy and exergy analysis". Proceedings of the18th International Congress of Mechanical Engineering, November 6-11, Ouro Preto, MG, CD-ROM, 8 pages.

Lipman, T., 2004, "What will power the hydrogen economy?" Technical Report UCD-ITS-RR-04-10, The Natural Resources Defense Council.

Matsuzaki, Y., Yasuda, I., 1999, "Relationship between the steady-state polarization of the SOFC air electrode, La0.6Sr0.4MnO3+δ/YSZ, and its complex impedance measured at the equilibrium potential", Solid State Ionics, 126 (3-4), pp. 307-313.

Morse, S., 2004, "Hydrogen – The Fuel of Today" Technical report. Available at www.eng.usf.edu/rnr/ret_2004/ HYDROGEN_FUEL_OF_THE_FUTURE.doc

Ogden, J.M., 2002, "Review of small stationary reformers for hydrogen production", Technical Report IEA/H2/TR-02/002, International Energy Agency

R. A. Roberts, F. Jabbari, J. Brouwer, G. S. Samuelsen, E. A. Liese, R. S. Gemmen. Inter-laboratory dynamic modeling of a carbonate fuel cell for hybrid application. In: International Gas Turbine Institute Meeting of the ASME. Atlanta, Georgia, June 16 – 19, 2003.

Simulink/MATLAB is a product of The Mathworks, 3 Apple Hill Drive, Natick, MA 01760-2098, USA. (http://www.mathworks.com/).

Sunde, S., 1997, "Calculations of impedance of composite anodes for solid oxide fuel cells", Electrochimica Acta, 42 (17), pp. 2637-2648.

Takehara, Z., Kanamura, K., Yoshioka, S., 1989, "Thermal energy generated by entropy change in solid oxide fue cell", Journal of the Electrochemical Society, 136 (9), pp. 2506-2512.

Tanner, C. W., Fung, K. Z., Virkar, A. V., 1997, "The effect of porous composite electrode structure on solid oxide fuel cell performance: I - theoretical analysis", Journal of the Electrochemical Society, 144 (1), pp. 21 - 30

Virkar, A. V., Chen, J., Tanner, C.W., Kim, J.W., 2000, "The role of electrode microstructure on activation and concentration polarizations in solid oxide fuel cells". Solid State Ionics. Vol. 131, pp. 189 - 198.

Vollmar, H.-E.; Maier, C.-U.; Nölscher, C.; Merklein, T.; Poppinger, M., 2000, "Innovative concepts for the coproduction of electricity and syngas with solid oxide fuel cells". Journal of Power Sources, Vol. 86, p. 90 – 97.